LIMNOLOGY
and
OCEANOGRAPHY: METHODS

ASLO

*Limnol. Oceanogr.: Methods* 15, 2017, 291–301

doi: 10.1002/lom3.10157

# SIPCO2: A simple, inexpensive surface water $pCO_2$ sensor

**Christopher W. Hunt,[1]* Lisle Snyder,[2] Joseph E. Salisbury,[1] Douglas Vandemark,[1] William H. McDowell[2]**
[1]Ocean Process Analysis Laboratory, University of New Hampshire, Durham, New Hampshire
[2]Department of Natural Resources and the Environment, University of New Hampshire, Durham, New Hampshire

## *Abstract*

Efforts to estimate air-water carbon dioxide ($CO_2$) exchange on regional or global scales are constrained by a lack of direct, continuous surface water $CO_2$ observations. Sensor technology for the in situ measurement of the partial pressure of carbon dioxide ($pCO_2$) has progressed, but still poses limitations including expense and biofouling concerns. We describe a simple, inexpensive, in situ $pCO_2$ method (SIPCO2) in which a non-dispersive infrared (NDIR) detector is paired with an air pump in an enclosed housing to produce air-sea equilibration. We first evaluated this approach in a laboratory setting, then in an estuarine-coastal ocean laboratory for several months to continuously monitor aquatic $pCO_2$. An accepted, accurate NDIR-based $CO_2$ measurement technique was employed alongside SIPCO2 to provide an assessment of sensor performance. SIPCO2 allows for low-cost, relatively accurate measurements of $pCO_2$ (mean difference of $-5 \pm 5$ $\mu$atm from validation system after laboratory calibration) without reagents or membranes, and can be assembled and operated with a minimal amount of technical skill. While not suitable for some exacting applications, this SIPCO2 approach could rapidly and effectively increase the number of quality $CO_2$ observations in a range of aquatic environments. We also provide detailed instructions for the assembly of SIPCO2 from commercially available components.

Recent examinations of the fluxes of carbon dioxide ($CO_2$) between the terrestrial, atmospheric, inland aquatic, estuary, and coastal ocean provinces have illustrated both their dynamic nature and importance to regional and global carbon budgets (Frankignoulle 1988; Raymond et al. 1997; Cole et al. 2007; Raymond et al. 2013; Signorini et al. 2013; Laruelle et al. 2014, 2015; Borges et al. 2015). Many of these studies, particularly those focused on inland waters, have not used direct observations of the partial pressure of carbon dioxide ($pCO_2$) in water, but instead have derived $pCO_2$ from other measures of the carbonate system for some or all of the analysis (Raymond et al. 1997; Cole et al. 2007; Atilla et al. 2011; Butman and Raymond 2011; McDonald et al. 2013; Laruelle et al. 2015). This derivation is commonly accomplished through the pairing of discrete total alkalinity and pH sample data (Park 1969), a technique which has been shown to result in a large potential overestimate of $pCO_2$ due to diverse factors such as interferences (particularly in freshwater systems) from non-carbonate contributions to alkalinity (Hunt et al. 2011; Wang et al. 2013; Abril et al. 2015) and electrode-based pH measurement errors in seawater (Hoppe et al. 2012; Bockmon and Dickson 2015).

*Correspondence: chunt@unh.edu

Additional Supporting Information may be found in the online version of this article.

While a more complete understanding of non-carbonate contributions to alkalinity could potentially lead to accurate indirect estimates of $pCO_2$ from discrete measurements—as could the pairing of sample measurements of dissolved inorganic carbon and pH—an alternative way to improve and constrain $CO_2$ budgets is to vastly increase the number of direct $pCO_2$ observations, especially in freshwaters where non-carbonate interferences are the most prevalent. The need for direct $pCO_2$ measurements, together with technological improvements, has resulted in a variety of innovative new $pCO_2$ sensor technologies. These technologies employ several equilibration techniques, including headspace equilibration through a gas-permeable membrane and non-membrane equilibration, as well as contrasting $CO_2$ detection techniques such as non-dispersive infrared (NDIR) detection and chemical reagent detection (Table 1). An evaluation of four commercial $pCO_2$ sensors in coastal waters by the Alliance for Coastal Technology in 2010 found a range of sensor performance compared to a documented underway-type $pCO_2$ system (using a membrane-based equilibrator and NDIR $CO_2$ detection, Hales and Takahashi 2004) and discrete $pCO_2$ measurements ($pCO_2$ derived from total alkalinity and pH). A separate evaluation of a membrane-equilibration technique compared sensor data to discrete headspace $CO_2$ measurements with a large range of reported sensor discrepancy (Johnson et al. 2010).

Although these commercial in-water measurement sensors are generally pre-configured for immediate use, they are also

**Table 1.** Aquatic $CO_2$ sensors and their performance characteristics.

| Manufacturer/ sensor | Measurement method | Range of difference from standard system (mean difference) | Standard deviation range | Citation |
|---|---|---|---|---|
| Contros Hydro-C | Pumped membrane equilibration, NDIR detection | −16 to +96 μatm | +/− 17 to 25 μatm | Alliance for Coastal Technologies (ACT) (2010*a*) |
| Pro-Oceanus $CO_2$-Pro | Pumped membrane equilibration, NDIR detection | +9 μatm | +/− 14 μatm | Alliance for Coastal Technologies (ACT) (2010*b*) |
| Vaisala CARBOCAP (modified) | Passive membrane equilibration, NDIR detection | +5 to +881 ppm* | Not reported | Johnson et al. (2010) |
| Sunburst SAMI-CO2 | Passive membrane equilibration, reagent-based colorimetry | +18 to +40 μatm | +/− 9 to 40 μatm | Alliance for Coastal Technologies (ACT) (2010*c*) |
| PMEL/Batelle MAPCO2 | Bubble equilibration, NDIR detection | −12 to +3 μatm | +/− 8 to 30 μatm | Alliance for Coastal Technologies (ACT) (2010*d*) |
| This study- before characterization | Pumped air equilibration, NDIR detection | +7 to +65 μatm† | +/− 6 μatm | This study |
| This study- after characterization | Pumped air equilibration, NDIR detection | −26 to +30 μatm‡ | +/− 6 μatm | This study |

* Converted from mg/L, assuming 0°C and 1.01325 bar pressure.
† SIPCO2 CML data without laboratory calibration applied.
‡ SIPCO2 CML data with laboratory calibration applied.

vulnerable to biofouling (especially in the case of membrane-type systems and the SAMI-$CO_2$ water intake tube), are sometimes complex to install due to multiple components requiring specialized mounting hardware (MAPCO2), and costly. Recently, Bastviken et al. (2015) presented a innovative design for a passively equilibrated $pCO_2$ sensor, using the same low-cost $CO_2$ detector employed in this study, with good detector linearity and promising results against discrete bottle-headspace $pCO_2$ measurements. These results indicate that these inexpensive detectors hold great potential for the construction of an in situ $pCO_2$ sensor. However, the bottle-headspace method has several shortcomings (Bastviken et al. 2015), and that study did not provide assessment of performance against a validated continuous headspace-equilibration system. Here, we present an alternative design for a simple, inexpensive $pCO_2$ sensor (SIPCO2) that can be assembled in a few hours from off-the-shelf or easily obtained components totaling less than $500 USD. We then present results from two evaluation exercises, the first a multi-day lab test in a tank of manipulated freshwater, the second a multi-month test at a coastal laboratory. While we emphasize and discuss how evaluation conditions differed between the SIPCO2 evaluations and those of commercially available sensors, and thus results may not be directly comparable, SIPCO2 performance was similar to that of the sensors listed in Table 1 once calibrated against an accepted $pCO_2$ measurement system.

## Materials and procedures

### Equilibration background

Among all styles of in-water $CO_2$ sensors, one common element is the necessity to separate aqueous $CO_2$ from the liquid medium into a measureable state. All the sensors in Table 1 measure $CO_2$ in the gaseous state via NDIR detection with the exception of the Sunburst SAMI-$CO_2$, which measures pH change in the liquid phase as $CO_2$ exchanges across a membrane (DeGrandpre et al. 1995). In marine $pCO_2$ observations the technique of equilibrating an air headspace with a water mass of interest has been used for decades (Takahashi 1961; Weiss 1981; Wanninkhof and Thoning 1993). According to this technique, after equilibration the gas composition of the headspace reflects that of the water mass. Often the equilibrator is a showerhead-type in which the air headspace is ultimately pumped to a NDIR detector at a set rate. The MAPCO2 system achieves equilibration through a combination of wave and bubble action, and components in contact with seawater are constructed of copper alloy to prevent biofouling (Friederich et al. 1995, ACT 2010). All types of equilibrators can be vulnerable to fouling, even those constructed using an anti-fouling agent such a copper, and must be cleaned often to maintain accurate $pCO_2$ measurements. More recently, use of this technique has migrated upstream to estuary and freshwater environments (Frankignoulle and Borges 2001; Abril et al. 2006). The underlying principle of this type of equilibration requires that a relatively large volume of water is exchanged with a relatively small air headspace to equilibrate the $CO_2$ levels between the two media. This concept requires the transfer via pumps of small volumes of air and larger volumes of water. Our design simplifies this concept by recirculating headspace air below the water surface via a small air pump; the resulting bubbles equilibrate $CO_2$ with the surrounding water, break, and the released air rises through

tubing or a pipe back to the headspace containing a small NDIR detector (Fig. 1). The same headspace air is recirculated, providing equilibration at a rate suitable for applications where: (1) the sample water is not rapidly changing its carbonate characteristics, and (2) bubbles do not escape the return pipe or the enclosure is not opened to ambient air.

**SIPCO2 sensor design**

The SIPCO2 sensor design (Fig. 1) has two electromechanical components—the air pump and NDIR detector—housed in an off-the-shelf plastic electrical junction box (component parts list included in Supporting Information Material). In order to maintain equilibration, the air pump is run continuously, although it may be possible to run the pump intermittently to conserve power, especially when powered by a battery. The flow rate of the selected pump is listed by the manufacturer (KNF Neuberger) as 0.45 L $min^{-1}$, with an operating life of 10,000 h for the brushless model, although in other applications we have observed pump durability of 4–5 yr.

The NDIR detector employed in this work was a SenseAir K-30 (ASCII model, SenseAir AB, Delsbo Sweden). The K-30 detector has a manufacturer-specified measurement range of 0–10,000 ppm $CO_2$, an accuracy of ± 30 ppm ± 3% of the measurement value, and a precision of ± 20 ppm ± 1% of the measurement value. Our own results found that with calibration the K-30 can achieve both better accuracy and better precision, as discussed below. The ASCII output version of the K-30 sensor used in this work provides an automatic ASCII-format $CO_2$ measurement every 2 s. A vendor-supplied control program ("Gaslab") was used to calibrate the K-30, although this program is limited to calibration concentrations of 0 and 400 ppm only. For both the laboratory evaluation and coastal laboratory evaluation discussed below, the SIPCO2 sensor was powered by a standard 5-volt Universal Serial Bus connection to a laptop computer. This computer also logged the ASCII SIPCO2 data output via a terminal program. The K-30 comes equipped with an onboard temperature sensor. While we performed a later evaluation of the temperature dependency of the K-30 (described below), the onboard temperature component failed during the two central evaluations of this work.

**Validation system**

The validation system, typically used for shipboard continuous-flow $pCO_2$ measurements (see Hunt et al. 2013) consisted of an equilibrator with spray nozzle, with headspace air recirculated by a small air pump between the equilibrator and a Li-cor LI-840 NDIR detector. The manufacturer-specified operating range of the LI-840 NDIR is 0–3000 ppm $CO_2$. The validation system was calibrated with ultrapure nitrogen and an 835 ppm $CO_2$/nitrogen mixture, and a computer-controlled system of valves flowed the same calibration gases through the validation LI-840 NDIR once every 3 h to check system calibration stability. The estimated uncertainty of the validation system is +/− 3 $\mu$atm (Vandemark et al. 2011).

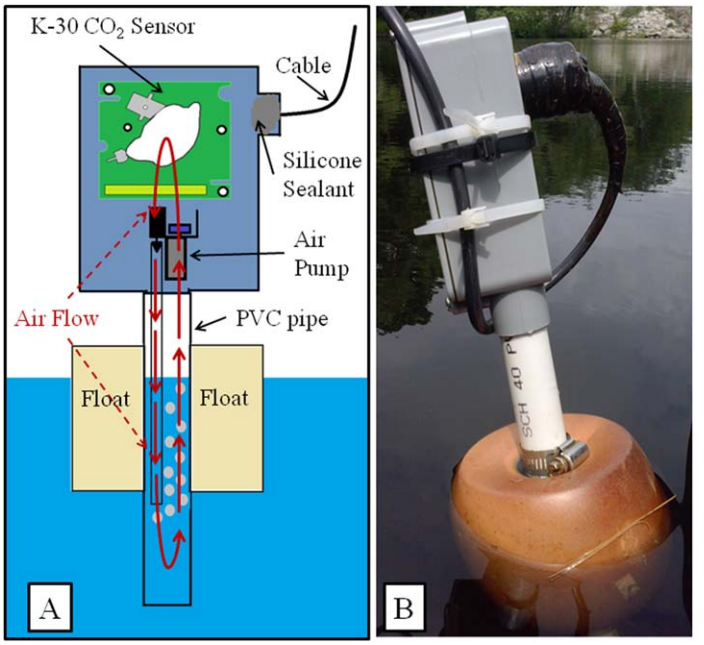


**Fig. 1.** Panel **A**: SIPCO2 sensor design. A components list is provided in the Supporting Information Material. Panel **B**: the prototype SIPCO2 sensor deployed in the Lamprey River, New Hampshire U.S.A.

**$pCO_2$ calculation**

The SIPCO2 K-30 detector reported measurements as the molar fraction of $CO_2$ ($xCO_2$). Since the sensor housing was open to the water surface, the readings reported by the SIPCO2 sensor were "wet" ($xCO_{2wet}$). These $xCO_{2wet}$ data were corrected to sea surface temperature, assuming the temperature inside the SIPCO2 was also equilibrated to the observed sea surface temperature, and converted from $xCO_{2wet}$ to the partial pressure of carbon dioxide ($pCO_2$, wet air), according to standard methods (Dickson et al. 2007), assuming the SIPCO2 headspace was at ambient atmospheric pressure, measured by a nearby meteorological array. In contrast, the sample stream of the validation system described above was drawn through tubing containing a Nafion selectively permeable membrane (Perma Pure, Toms River, New Jersey), which dried the sample gas stream of water vapor, resulting in validation system readings of $xCO_{2dry}$. These $xCO_{2dry}$ validation data were corrected to sea surface temperature and converted from $xCO_{2dry}$ to $pCO_2$ as above (Dickson et al. 2007). Thus, all $pCO_2$ data presented in this work are in the form of partial pressures of $CO_2$ in wet air.

**Laboratory evaluation**

The K-30 detector was initially removed from the SIPCO2 housing and calibrated in the lab by placing the sensor in a

sealed plastic bag with a small opening for gas tubing and detector cable. When gas flow was introduced the positive pressure flushed the bag after several minutes, allowing for stable $CO_2$ readings from the detector. The detector was zeroed with ultrapure nitrogen, then subsequently spanned with a 400 ppm $CO_2$/nitrogen mixture. The limitations of this detector calibration procedure are discussed later in this work. After calibration, the K-30 detector was placed into the sensor housing and run in the lab continuously for several days alongside a more traditional aquatic $CO_2$ system. Both $pCO_2$ systems measured a tank of ~ 200 L tap water, with the SIPCO2 sensor placed directly into the tank, while water was recirculated between the tank and validation system's equilibrator via a submersible pump. The temperature of the SIPCO2 headspace was assumed to be equal to that of the water in the tank. The simultaneous use of the SIPCO2 and validation systems allowed us to compare the behavior of the SIPCO2 sensor over a wider range of $CO_2$ in the lab, as carbonated water was added to the tank twice to raise $CO_2$ levels (Fig. 2). These carbonated water additions also allowed the estimation of the SIPCO2 sensor response time.

**Coastal marine laboratory evaluation (CML)**

A longer-term sensor evaluation was conducted from 22 November 2014 to 12 March 2015 at the University of New Hampshire Coastal Marine Laboratory (CML), a facility at the mouth of the Piscataqua River, which drains to the coastal Gulf of Maine (43.0°N 70.7°W). The facility has a continuous seawater supply, pumped from near the bottom of the adjacent channel at a tide-varying depth between 4.5 m and 7 m. The same sensor used in the laboratory evaluation, which was not recalibrated following the laboratory evaluation, was placed into a ~ 200 L tank similar to that used in the laboratory evaluation, which was continuously flushed with seawater at an approximate rate of 10 L/min. The CML tank also contained a thermosalinograph (Aanderaa 4319B), which collected data for 10 min each hour. Salinities reported in this paper are on the PSS-78 scale (Lewis 1980). A separate seawater line continually supplied the headspace gas equilibrator for the CML $CO_2$ seawater measurement system. This system was identical to that used in the laboratory evaluation, and measurements of ultrapure nitrogen and an 835 ppm $CO_2$/nitrogen mixture were made every 4 h to determine the stability of the validation system. While the SIPCO2 and validation $CO_2$ systems were run continuously, only the $pCO_2$ data from these systems collected over the 10-min period when the thermosalinograph was in operation were used to produce 10-min average values once per hour, which comprise the dataset presented here.

## Assessment

**Laboratory evaluation**

During the laboratory evaluation, the SIPCO2 sensor closely tracked the validation system during unperturbed periods ($r^2 = 0.99$). Shortly after two rapid additions of $CO_2$ the SIPCO2 sensor response lagged that of the validation system (Fig. 2). Results of mean offsets ($Off_{mean}$, calculated as differences between sensor readings, Eq. 1) show that readings from the SIPCO2 sensor were consistently higher than those from the validation system (excepting the periods of rapid $CO_2$ increase during the two perturbation periods). This consistent offset was present despite the calibration of the SIPCO2 NDIR detector with the same gas standards used to calibrate the validation system (Table 2).

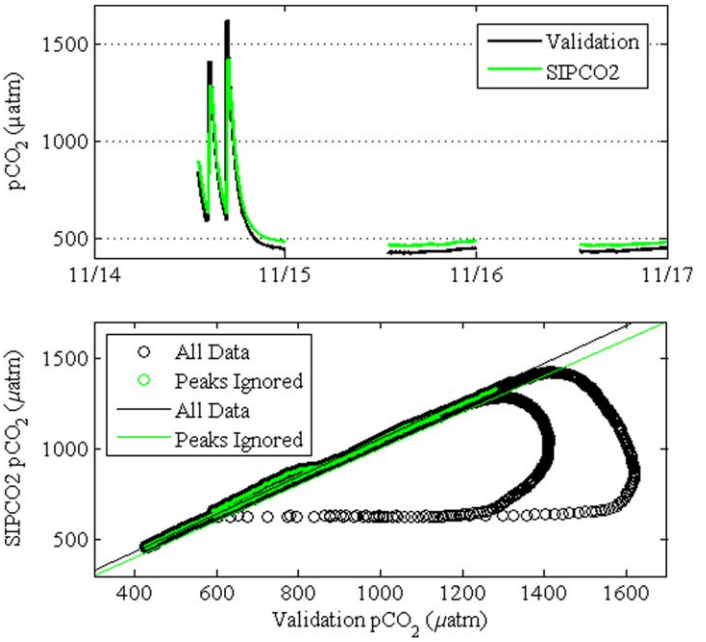


**Fig. 2.** Laboratory SIPCO2 sensor evaluation. Top panel: timeseries plot of SIPCO2 and validation system $pCO_2$ measurements. Difficulties with the K-30 $CO_2$ sensor logging software, which reset at the end of each day, resulted in the data gaps shown. Bottom panel: scatterplot of SIPCO2 $pCO_2$ readings against validation system $pCO_2$ readings, including two $CO_2$ additions (green points) and excluding $CO_2$ additions (black points).

$$\mathrm{Off}_{\mathrm{mean}} = \frac{1}{n} * \sum_{i=1}^{n} (\mathrm{pCO_2\ SIPCO2} - \mathrm{pCO_2\ Validation}) \quad (1)$$

There is a substantial discrepancy between the mean offsets if data from the perturbation periods are included (Table 2). Standard deviations of the mean offsets (calculated as in Eq. 2) show that the perturbation periods represented a large amount of variance, while ignoring these periods yielded a standard deviation (precision) of ± 14 µatm. A ± 14 µatm precision, which translates to a ± 3.5% relative uncertainty at a $pCO_2$ of 400 µatm, represents an unacceptable level of uncertainty for exacting applications; for instance, this uncertainty exceeds the desired levels of both the "weather" and "climate" objectives (2.5% and 0.5% desired

**Table 2.** Offset and linear regression results of the laboratory evaluation of the SIPCO2 sensor.

| | With peaks | Without peaks |
|---|---|---|
| $Off_{mean}$ ($\mu$atm) | 30.2 ($\pm$76.7) | 42.7 ($\pm$14.2) |
| Slope | 0.88 | 1.03 |
| Intercept | 105 | 22 |
| $R^2$ | 0.92 | 0.99 |

uncertainty, respectively) of the Global Ocean Acidification Observing Network (GOA-ON, Newton et al. 2015).

$$Off_{std} = \sqrt{\frac{1}{n}\sum_{i=1}^{n}(pCO_{2\ SIPCO2} - pCO_{2\ Validation})^2} \quad (2)$$

Linear regressions of the SIPCO2 sensor readings against those from the validation system, both for the entire comparison period and for the two periods without $CO_2$ additions are listed in Table 2. The response time of the SIPCO2 system lagged that of the validation system, resulting in the separation of the two peaks in Fig. 2 (top panel) and deviation from linearity apparent in Fig. 2 (bottom panel). The time lag between the highest validation system $pCO_2$ and SIPCO2 $pCO_2$ was approximately 9 min for the first peak, and 11 min for the second peak, indicating a slower response time for the SIPCO2 sensor. The validation system responded quickly to the $CO_2$ additions (less than one minute from initial addition to the start of the validation system response), while 3 min and 4 min elapsed between the start of the validation response to peak validation $pCO_2$), resulting in total validation system response times of 4 and 5 min for the first and second peaks, respectively. Addition of these validation system response times with the 9 min and 11 min lags between the validation and SIPCO2 peaks, together with a 1 min lag between the $CO_2$ addition and start of validation system response, results in a conservative SIPCO2 response time estimate of 15 min. The highest SIPCO2 readings for the two peaks (1284 $\mu$atm and 1421 $\mu$atm, respectively) were lower than those from the validation system (1411 $\mu$atm and 1618 $\mu$atm, respectively), suggesting that the added $CO_2$ from the carbonated water escaped the tank quickly enough that the SIPCO2 sensor could not fully equilibrate due to the slower SIPCO2 sensor response time. This is probably due in part to the rapid recirculation of water through the validation system's equilibrator; thus, we might expect a slower $CO_2$ decrease in naturally less-turbulent waters.

We performed a linear regression of the SIPCO2 sensor readings against those from the validation system to examine the linear response of the SIPCO2 sensor (Table 2; Fig. 2). When the peaks from the $CO_2$ additions were excluded, the SIPCO2 sensor response was quite linear to that of the validation system ($r^2 = 0.99$), with a near 1 : 1 slope.

**Table 3.** Summary of hydrographic conditions and $pCO_2$ observations from the Coastal Marine Lab evaluation. Min is the minimum measurement during the evaluation, Max is the maximum measurement observed, SD is the standard deviation of the measurement during the evaluation ($n = 2{,}539$ hourly means).

| | Mean | Median | Min | Max | SD |
|---|---|---|---|---|---|
| Salinity | 29.95 | 30.45 | 22.31 | 32.28 | 1.87 |
| Water temperature | 4.31 | 4.85 | −0.75 | 10.39 | 2.93 |
| Dissolved oxygen ($\mu$mol 1-1) | 345 | 338 | 269 | 433 | 33 |
| Validation $pCO_2$ | 402 | 399 | 338 | 472 | 27 |
| K-30 $pCO_2$ | 431 | 430 | 360 | 501 | 30 |

**Coastal marine laboratory evaluation**

Hydrographic conditions at the CML varied over the approximately three and a half months the SIPCO2 sensor was deployed (Table 3). Water temperatures gradually decreased from 10°C to near 0°C as the season progressed from late fall to winter, then began to rise at the end of the evaluation in spring. Salinity reached a minimum in late December due to higher than normal rainfall. Underlying these seasonal changes were clear semi-diurnal tidal signals, with high tide bringing warmer water temperatures and higher salinities. The magnitudes of salinity and temperature changes varied with lunar phase, as well as with precipitation and associated changes in freshwater input, but water temperature generally varied 1–2°C between low and high tides, while salinity varied 1.5–3.

As in the laboratory evaluation, the SIPCO2 sensor sensitively tracked the readings of the validation $pCO_2$ system at the CML, but with somewhat higher readings (Fig. 3; Tables 2, 4). The offset between the SIPCO2 sensor and validation system (Fig. 3, bottom panel) varied from 7 $\mu$atm to 65 $\mu$atm over the CML test, with a mean offset of 29 $\mu$atm and standard deviation of 6 $\mu$atm (Table 4). This mean offset from the CML evaluation is somewhat lower than the mean offset found in the laboratory evaluation (42.7 $\mu$atm, without peaks), but within one standard deviation of the laboratory evaluation mean (Table 2). Paired *t*-tests show that the mean CML offset is significantly different than the mean laboratory evaluation offset at the 95% significance level. The results of a linear regression of the SIPCO2 readings against those from the validation system at the CML yielded slightly different slopes than observed in the laboratory evaluation (1.08 $\mu$atm and 1.03 $\mu$atm, respectively), as well as different intercepts (−1.9 $\mu$atm and 22 $\mu$atm, respectively).

**Coastal marine laboratory evaluation data correction**

We used the results of the laboratory evaluation results in two ways to attempt to correct the SIPCO2 sensor readings

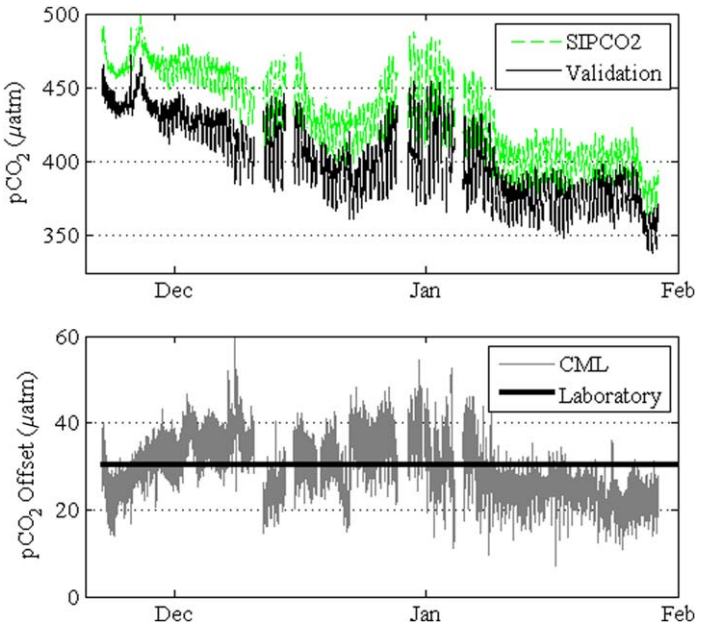


**Fig. 3.** Comparison data collected at the UNH Coastal Marine Lab. Top panel: time series of $pCO_2$ readings from SIPCO2 and validation systems. Data gaps in this panel are due to the removal of data when the validation system equilibrator was clogged. Bottom panel: time series of sensor offsets, with the mean offset from the laboratory evaluation shown as a solid line. Offsets were calculated as the difference between SIPCO2 and validation system measurements.

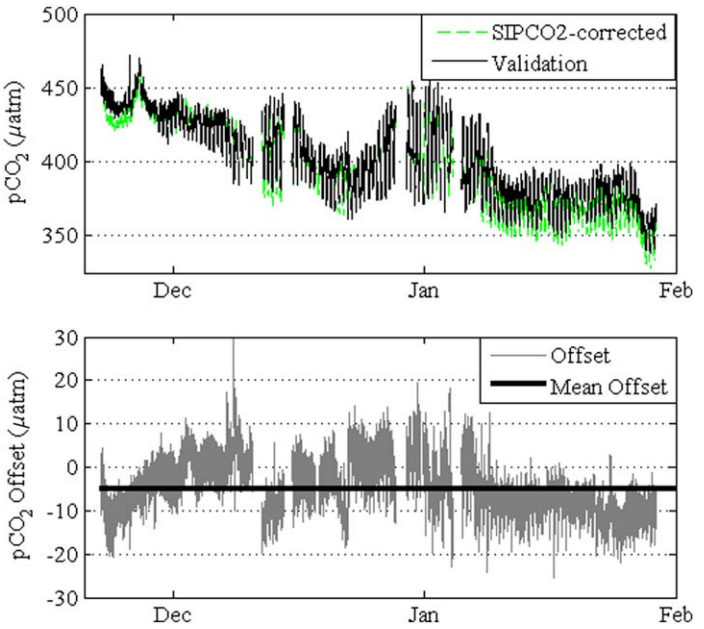


**Fig. 4.** Corrected comparison data collected at the UNH Coastal Marine Lab. Top panel: time series of corrected SIPCO2 sensor and validation system readings. The SIPCO2 correction was derived from the laboratory evaluation results (Eq. 3). Bottom panel: time series of sensor offsets, with the mean offset from the coastal laboratory evaluation ($-5$ $\mu$atm) shown as a solid line. Linear regression of the corrected CML SIPCO2 sensor data against validation system readings results in an equation of $pCO_{2\ SIPCO2} = 1.08*pCO_{2\ validation} - 30.8$, with a $r^2$ of 0.969 and $p \ll 0.001$.

**Table 4.** Offsets and regressions of uncorrected and corrected data from the CML SIPCO2 sensor test. Offsets were calculated as $pCO_{2\ SIPCO2}$ - $pCO_{2\ validation}$. The laboratory offset applied was 42.7 $\mu$atm (without peaks). The laboratory calibration applied to the data was that derived from the linear regression of data from the initial laboratory evaluation: $pCO_{2\ SIPCO2\ corrected} = (pCO_{2\ SIPCO2\ measured} - 22)/1.03$.

| | SIPCO2 uncorrected data | SIPCO2 laboratory offset applied | SIPCO2 laboratory calibration applied |
|---|---|---|---|
| $Off_{mean}$ ($\mu$atm) | 29 ($\pm$6) | $-$13.8 ($\pm$6) | $-$5 ($\pm$5) |
| Slope | 1.08 | 1.04 | 1.04 |
| Intercept | $-$1.9 | $-$23.5 | $-$23 |
| $R^2$ | 0.97 | 0.97 | 0.97 |

at the CML site. First, we used a simple offset removal, subtracting 42.7 $\mu$atm from the SIPCO2 sensor readings at the CML (Table 4). This offset correction lowered the mean CML offset to $-13.8 \pm 6$ $\mu$atm, which is closer to an ideal offset of 0 $\mu$atm. Second, we used the results of the linear regression of the laboratory evaluation and applied the same slope and intercept to the CML SIPCO2 sensor data (Table 4), according to Eq. 3:

$$pCO_{2\ corrected} = \frac{(pCO_{2\ SIPCO2} - 22)}{1.03} \quad (3)$$

This simple application of the slope and intercept from linear regression of the laboratory evaluation data produced the best SIPCO2 results from the CML (Fig. 4), bringing the mean offset to $-5 \pm 5$ $\mu$atm.

## Discussion

For many $pCO_2$ measurement applications in estuaries, lakes, or rivers, a SIPCO2 accuracy and precision of $29 \pm 6$ $\mu$atm, as determined in the CML evaluation, or $42.7 \pm 14.2$ $\mu$atm in the case of the laboratory evaluation, may be acceptable for examinations of air-water $CO_2$ fluxes or aquatic ecosystem metabolism; however, it is important to acknowledge that $pCO_2$ levels and ranges of variation in freshwater and estuary systems can be several times to an order of magnitude larger than the range tested in the CML evaluation. For instance, Abril et al. (2006) showed precision of directly measured river $pCO_2$ of $\pm$ 15% over a 0–13,000 ppm range. Borges et al. (2015) documented a method precision of $\pm$ 2% for IRGA-based direct measurements of African rivers ranging in $pCO_2$ from 300 ppm to 16,942 ppm. Hanson et al. (2003) determined net ecosystem productivity via IRGA-based $pCO_2$

measurements in 25 lakes, with an estimated $pCO_2$ precision of ± 2% over a 0–20,000 ppm range. Raymond et al. (1997) showed a precision of ± 8% over a range of about 500–2000 ppm in the tidal Hudson River estuary. Although the SIPCO2 level of accuracy and precision may be unacceptable for "climate" quality oceanic studies, the precision of results from the CML evaluation (± 6 μatm) exceeds the "weather" target uncertainty of ± 10 μatm (± 2.5% at 400 μatm $pCO_2$), but falls short of the "climate" target uncertainty of ± 2 μatm (± 0.5% at 400 μatm $pCO_2$, Newton et al. 2015). Furthermore, we have found that a pre- (and perhaps post-) deployment laboratory calibration may offer a way to improve the data quality from the SIPCO2 sensor.

We anticipate that a longer laboratory evaluation period with larger and more gradual $pCO_2$ changes than shown here will produce a more robust regression calibration. Thus, while a simple offset subtraction improved the SIPCO2 sensor readings at the CML site, the generation of a linear regression relationship against readings from a validation system appears to be a reasonable way to correct readings from this SIPCO2 sensor. It is worth noting that the CML evaluation spanned $pCO_2$ levels of a fairly narrow range (340–500 μatm). Freshwater field evaluations and verification of the linearity of the SIPCO2 sensor response are presently underway. Preliminary results indicate that the SIPCO2 sensor works well in the elevated pCO2 environment found in local rivers, where a wider range of $pCO_2$ is expected. This is consistent with the K-30 measurement specifications of Bastviken et al. (2015). The results of Bastviken et al. (2015) indicate that corrections for detector temperature and relative humidity offer additional ways to improve the quality of $CO_2$ readings from the K-30 NDIR detector, but we expect humidity impacts to be low for the SIPCO2 sensor due to typical operation at ~ 100% humidity in continuous mode. While Bastviken et al. (2015) noted problems with condensation, no condensation was observed in the SIPCO2 housing during these tests.

**Potential sources of error and uncertainty**

The consistent presence of an offset between SIPCO2 readings and those of the validation $pCO_2$ system (+42.7 μatm in the laboratory evaluation, Table 2, and + 29 μatm in the CML test, Table 4) suggest that there are additional sources of error in the SIPCO2 system. If quantified, knowledge of these errors could be used to improve the SIPCO2 data quality. Due to its simple design, the SIPCO2 system has two components which can create potential sources of error: the air pump and the K-30 NDIR detector. Faults in the air pump would result in incomplete equilibration or slower response times. While the response of the SIPCO2 lags that of the validation system (Fig. 2), an increase in this lag on the order of minutes may have produced a smaller offset, as shown by the difference between the $Off_{mean}$ values with and without peaks shown in Table 2. The air pump used in both the Laboratory and CML evaluations was not observed to have failed or exhibited reduced flow rates.

The K-30 NDIR detector is a more likely source of error in the SIPCO2 design. We performed three tests on a new K-30 NDIR sensor: linearity of response, temperature response, and humidity response. This K-30 module was not the same as used in the laboratory and CML evaluations, but was the same model and was prepared and calibrated with UHP $N_2$ and 400 ppm $CO_2$ in the same manner as described above. Similar to Bastviken et al. (2015), we compared the response of the K-30 NDIR to that of a Li-cor LI-840 NDIR, the same highly linear model used in the laboratory and CML evaluations of the SIPCO2 sensor. This response test was performed by mixing streams of ultrapure nitrogen and pure $CO_2$ with a valve to produce mixtures from 0 ppm to near-10,000 ppm $CO_2$, then flowing the mixed gas stream sequentially through the LI-840 and K-30 NDIR detectors, which were connected by short lengths of tubing. Results of this linearity test show that the response of the K-30 NDIR is linear ($r^2 = 0.9998$, Fig. 5). However, the slope of the regression line between K-30 and LI-840 NDIR detectors indicates that the K-30 NDIR underestimates $xCO_2$ at higher concentrations (slope = 0.93). This is a somewhat different finding than that presented by Bastviken et al. (2015), who showed a linear response from the K-30 NDIR but used a comparison NDIR (Los Gatos Research DLT100) that exhibits quenching effects and nonlinear behavior at higher $CO_2$ concentrations. At 350 μatm $pCO_2$, the approximate minimum reading during the CML evaluation, this translates to an offset of −26 μatm (calculated according to Eq. 1), while at 500 μatm $pCO_2$ the calculated offset is −36 μatm. The fact that this response linearity offset is negative (i.e., LI-840 readings are higher than K-30 readings), while the overall $Off_{mean}$ results from the laboratory and CML evaluations were positive indicates that another factor was more than offsetting the differences in response linearity between the two NDIR detectors. This finding indicates that calibration of a K-30 NDIR with mixtures of gases may not be sufficient to quantify the overall performance of a SIPCO2 sensor, and comparison to a validation system such as the one discussed here is advisable for highly accurate results.

Other studies examining the K-30 NDIR have demonstrated that the detector is sensitive to temperature and humidity changes (Yasuda et al. 2012; Bastviken et al. 2015). To examine the temperature response of the K-30 NDIR, we first calibrated the sensor at 20°C using ultra-high purity (UHP) nitrogen and 400 ppm $CO_2$ in nitrogen. We then flowed either UHP nitrogen or a 515 ppm mixture of $CO_2$ in nitrogen through the K-30 NDIR while altering the temperature of the K-30 detector. The temperature was altered by placing the K-30 NDIR on a chilled laboratory hot plate, which has previously been kept in a freezer. Contact between the K-30 NDIR and the chilled hot plate lowered the temperature of the K-30 to 5–10°C; the hot plate was then slowly warmed to

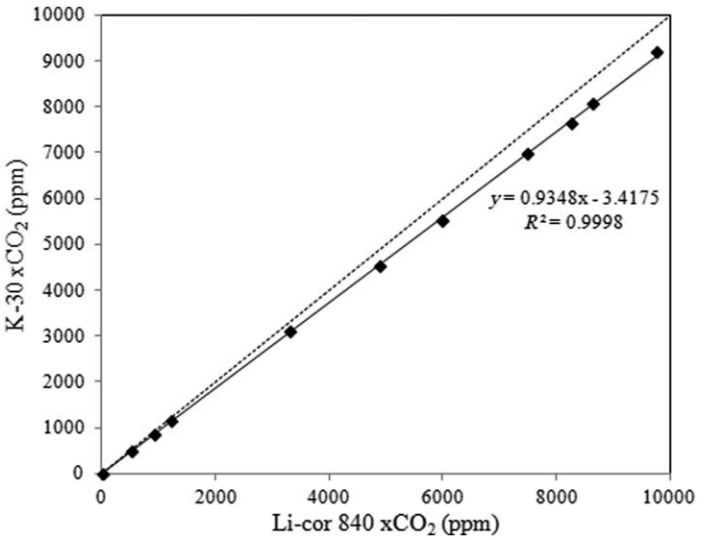


**Fig. 5.** Comparison of $xCO_2$ response between a Li-cor LI840 NDIR and a K-30 NDIR of the same model used in the SIPCO2 sensor. Standard deviation error bars in both the *x*- and *y*-directions are too small to appear in the plot. The dashed line indicates a 1 : 1 response, while the solid line shows the regression line between LI840 and K-30 detectors.

30–50°C, and the $xCO_2$ response of the K-30 NDIR was recorded (Fig. 6). The change in $xCO_2$ reading from temperature change was nearly identical between UHP nitrogen and 515 ppm $CO_2$. $xCO_2$ readings from the K-30 NDIR increased at temperatures greater than the calibration temperature (20°C), and fell below the known gas concentration at temperatures less than 20°C.

The K-30 NDIR has an onboard temperature sensor, and provides a detector temperature reading as part of its typical data stream. This offers the potential opportunity to temperature-correct the $xCO_2$ readings from a K-30 NDIR, using the logarithmic regression equation presented in Fig. 6. While Bastviken et al. (2015) noted a lack of temperature effect on K-30 readings, the equation shown in Fig. 6 is quite similar to the linear correction presented in Yasuda et al. (2012), a study in which several identical K-30 sensors were evaluated simultaneously.

To test the effect of varying humidity on K-30 NDIR readings, we employed a Li-cor 610 portable dew point generator. UHP nitrogen and the same 514 ppm $CO_2$ mixture employed above were flowed through the LI-610 instrument set to a dew point of 0°C, then subsequently to the K-30 NDIR sensor. The LI-610 was then adjusted to gradually increase the dew point of the UHP nitrogen or 514 ppm $CO_2$ mixture, while readings from the K-30 sensor were recorded. This test showed increasing $xCO_2$ readings from the K-30 sensor for UHP nitrogen, while the 514 ppm $CO_2$ mixture showed an initial slight $xCO_2$ decrease, followed by an $xCO_2$ increase above a dew point of about 10°C (Fig. 7). The temperature of the K-30 NDIR did not change appreciably over

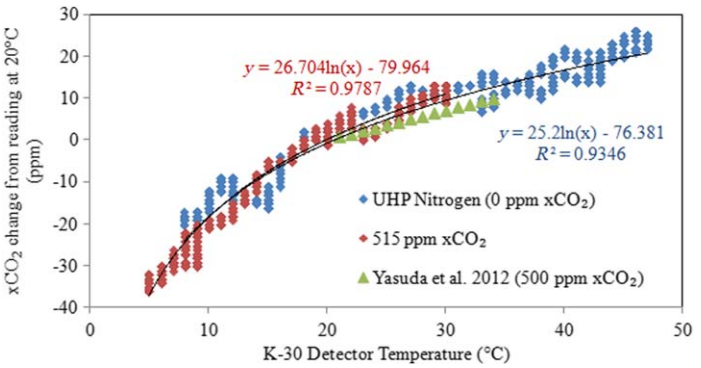


**Fig. 6.** Change in K-30 NDIR readings of a constant sample gas stream with varying temperature. Changes in UHP $N_2$ gas (0 ppm $xCO_2$) are shown in blue, while those of a 515 ppm $CO_2/N_2$ mixture are shown in red. The K-30 NDIR was calibrated at 20°C. Results from Yasuda et al. (2012) are shown in green, also for a K-30 NDIR calibrated at 20°C. The black line shows a logarithmic regression of the combined UHP $N_2$ and 515 ppm $CO_2/N_2$ data.

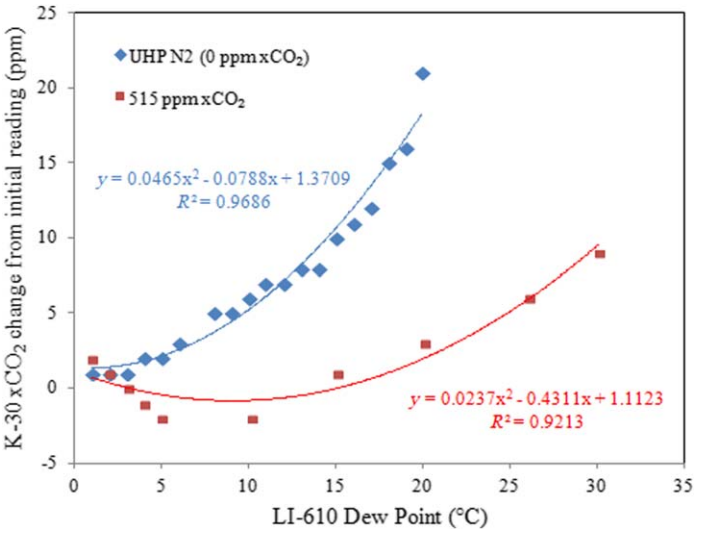


**Fig. 7.** Response of a K-30 NDIR detector to humidity change produced by a Li-cor LI-610 dew point generator. Blue points show changes in $xCO_2$ readings for UHP $N_2$ gas (0 ppm $xCO_2$), while red points show $xCO_2$ changes for a 515 ppm $CO_2/N_2$ mixture. Second-order polynomial regression lines and equations are shown in blue and red for the UHP $N_2$ gas and 515 ppm $CO_2/N_2$ mixture, respectively.

either dew point test, indicating that changes in $xCO_2$ readings were due solely to humidity. The manufacturer of the K-30 NDIR also offers models with onboard relative humidity measurements (i.e., K-33 ELG), the use of which offer the potential to correct for both temperature and humidity effects. While these models are somewhat more expensive, the capability to perform both temperature and humidity corrections would likely be valuable, particularly if the SIPCO2 sensor is to be deployed outside under a wide range of environmental conditions.

In light of these error sources, we can speculate whether some combination of the systematic K-30 underestimate of $xCO_2$ (Fig. 5), temperature effects (Fig. 6), and humidity effects (Fig. 7) can explain much of the $Off_{mean}$ determined in both the laboratory and CML evaluations (Tables 2, 4). Unfortunately, the temperature detector in the SIPCO2 K-30 used in both laboratory and CML evaluations malfunctioned, making post-correction of the data impossible. However, we can estimate what the potential effects would be at some likely temperatures, with a few assumptions. First, we assume that the air inside the SIPCO2 was at 100% humidity, as it was constantly recirculated beneath the water's surface by the air pump while remaining isolated from surrounding ambient air. Second, both the laboratory and CML evaluations were performed inside temperature-controlled buildings (although the CML building was generally colder), so we assume the air temperature inside the SIPCO2 was between 15°C and 25°C. Given these assumptions, the contribution of humidity to the observed $Off_{mean}$ should have been small (0 $\mu$atm at 15°C to 5 $\mu$atm at 25°C). Similarly the temperature contribution to the observed $Off_{mean}$ should also have been small ($-8$ $\mu$atm at 15°C to 5 $\mu$atm at 25°C, given a K-30 calibration temperature of 20°C). As previously discussed, at the minimum CML evaluation $pCO_2$ of 350 $\mu$atm the linearity offset is $-26$ $\mu$atm (calculated according to Eq. 1), while at 500 $\mu$atm $pCO_2$ the offset is $-36$ $\mu$atm. Combining linearity and humidity errors yields a net error offset ranging from $-44$ $\mu$atm (at 15°C and 500 $\mu$atm) to $-16$ $\mu$atm (at 25°C and 350 $\mu$atm). Under the above assumptions, the detector temperature would have to be 183°C to account for the linearity error, humidity error, and observed $Off_{mean}$ at 350 $\mu$atm, while the temperature would have to be 284°C to account for the same errors at 500 $\mu$atm. These results indicate that factors other than linearity, temperature, and humidity are producing the observed $Off_{mean}$; the results also underscore the importance of a careful evaluation of a SIPCO2 system against a validation system before attempting to make accurate measurements.

**Comparison to other $pCO_2$ sensors**

The $pCO_2$ readings from the SIPCO2 sensor before post-deployment adjustment underperformed some commercial sensors. For example, Degrandpre et al. (1995) demonstrate a SAMI-$CO_2$ accuracy/precision of $\pm 2$ $\mu$atm and $\pm 1$ $\mu$atm, respectively, although an intercomparison with a NDIR-based equilibrator system resulted in an overall offset between the two systems of 3.7 $\mu$atm. In comparison to a NDIR-based equilibrator system, Fietzek et al. (2013) found a Contros Hydro-C offset and precision of $-0.6$ $\mu$atm and $\pm 3$ $\mu$atm, respectively. However, after careful characterization against a validation system the SIPCO2 sensor performance is comparable to that of some of the systems presented in Table 1. The sensors discussed in the ACT evaluations: Contros Hydro-C (Fietzek et al. 2013), Pro-Oceanus $CO_2$-Pro, Sunburst SAMI-$CO_2$ (Degrandpre et al. 1995), and PMEL/Batelle MAPCO2 (Friederich et al. 1995) were tightly restricted, while we had continuous access to the SIPCO2 system, so this work does not present an evaluation conducted under directly comparable conditions to many of the sensors listed in Table 1.

The presented SIPCO2 sensor configuration ($200USD to $500USD for sensor components, see Supporting Information Material) offers a significant price advantage in comparison to the commercial systems described in Table 1. One disadvantage of the SIPCO2 sensor is an assembly time of several hours combined with a further time requirement to evaluate sensor performance, as opposed to an off-the-shelf system. However, we also believe the SIPCO2 configuration, using a small air pump to recirculate air within a small housing, offers a reduced risk of biofouling or sensor damage when compared to sensors that employ a membrane to exchange $CO_2$. Another advantage of the SIPCO2 design is the modular nature of the sensor, which allows for the easy replacement of components that may fail over time.

One disadvantage of the SIPCO2 sensor as described here is its response time, which is somewhat slow in comparison to other commercial sensors (on the order of 10 min in the laboratory evaluation). The use of a more powerful air pump to provide a higher flow rate should mitigate this issue, although we have not tested this possibility. The results in this work suggest that the SIPCO2 sensor could support many fixed-location scientific and monitoring applications, as opposed to use as a portable handheld $pCO_2$ sensor such as described in Johnson et al. (2010). Interestingly, Bastviken et al. (2015) show a negligible difference in $pCO_2$ readings between pumped and unpumped systems, although their measurement timescale was on the order of several hours. Further investigation into response time and mixing rates is warranted depending on specific application needs.

A key issue in the use of the SIPCO2 sensor relates to calibration. The host software for the K-30 $CO_2$ detector used in the SIPCO2 sensor at present only allows calibrations with gases of zero and 400 ppm $CO_2$. This is a relatively narrow calibration range for many applications, as $pCO_2$ can range an order of magnitude or higher in aquatic systems (Raymond et al. 1997; Hunt et al. 2013; Bastviken et al. 2015). While Bastviken et al. (2015) and results in this work show good K-30 sensor linearity, this limited K-30 calibration range underscores the need to characterize the SIPCO2 system against a validation system in a variety of environments.

Because the SIPCO2 sensor housing is not completely sealed from the environment, the present design is not submersible, and thus is only useful for surface measurements or integrated measurements of $pCO_2$ down to the depth of the pump's air tubing. Furthermore, this version has no ability to log data internally or operate autonomously on battery power. However, the cost, ease of assembly, and quality of

data suggest that the SIPCO2 provides a potentially valuable instrument for observation nodes in freshwater, estuary, and coastal environments. The addition of low-cost components could readily address data-logging and power issues. The SIPCO2 sensor represents a basic platform for aquatic $pCO_2$ measurements, to which users could add functionality to suit individual needs and requirements.

## Comments and recommendations

This paper presents a new design for a relatively inexpensive sensor to measure aquatic $pCO_2$ from readily obtainable components, evaluates the performance of the sensor in two settings, and provides a simple method to correct the sensor data against a known validation system. Uncorrected SIPCO2 sensor performance is below that of comparable commercial sensors ($30 \pm 6$ $\mu$atm difference from validation system), but post-deployment correction of the SIPCO2 measurements produces data of comparable quality ($-5 \pm 5$ $\mu$atm difference from validation system).

While many researchers may prefer out-of-the-box sensors for their application, we expect that the open design and cost savings of the SIPCO2 sensor will make it appealing to many users. The supplementary material provides a list of SIPCO2 sensor components, suppliers for many of the components, as well as step-by-step instructions for assembly. We strongly recommend calibration of the SIPCO2 sensor against a known validation system in order to produce the highest quality data possible. One potentially powerful use of this sensor is within a network of observation nodes, where numerous sensors could be deployed spatially around a validation system. This could dramatically increase the extent of in situ $pCO_2$ coverage while assuring data quality using a single expensive validation system.

## References


Abril, G., S. Richard, and F. Guérin. 2006. In situ measurements of dissolved gases (CO2 and CH4) in a wide range of concentrations in a tropical reservoir using an equilibrator. Sci. Total Environ. **354**: 246–251. doi:10.1016/j.scitotenv.2004.12.051

Abril, G., and others. 2015. Technical Note: Large overestimation of pCO2 calculated from pH and alkalinity in acidic, organic-rich freshwaters. Biogeosciences **12**: 67–78. doi:10.5194/bg-12-67-2015

Alliance for Coastal Technologies (ACT). 2010*a*. Performance Demonstration Statement for Contros HydroC$^{TM}$/CO2, ACT DS10-01 UMCES/CBL 10-091.

Alliance for Coastal Technologies (ACT). 2010*b*. Performance Demonstration Statement for Pro-Oceanus Systems Inc. PSI $CO_2$-Pro$^{TM}$, ACT DS10-03 UMCES/CBL 10-093.

Alliance for Coastal Technologies (ACT). 2010*c*. Performance Demonstration Statement for Sunburst Sensors SAMI-$CO_2$, ACT DS10-04 UMCES/CBL 10-094.

Alliance for Coastal Technologies (ACT). 2010*d*. Performance Demonstration Statement for PMEL MAPCO$_2$/Battelle Seaology $pCO_2$ Monitoring System, ACT DS10-02 UMCES/CBL 10-092.

Atilla, N., G. A. McKinley, V. Bennington, M. Baehr, N. Urban, M. DeGrandpre, A. R. Desai, and C. Wu. 2011. Observed variability of Lake Superior pCO2. Limnol. Oceanogr. **56**: 775–786. doi:10.4319/lo.2011.56.3.0775

Bastviken, D., I. Sundgren, S. Natchimuthu, H. Reyier, and M. Gålfalk. 2015. Technical Note: Cost-efficient approaches to measure carbon dioxide (CO2) fluxes and concentrations in terrestrial and aquatic environments using mini loggers. Biogeosciences **12**: 3849–3859. doi:10.5194/bg-12-3849-2015

Bockmon, E. E., and A. G. Dickson. 2015. An inter-laboratory comparison assessing the quality of seawater carbon dioxide measurements. Mar. Chem. **171**: 36–43. doi:10.1016/j.marchem.2015.02.002

Borges, A. V., and others. 2015. Globally significant greenhouse-gas emissions from African inland waters. Nat. Geosci. **8**: 637–642. doi:10.1038/ngeo2486

Butman, D., and P. A. Raymond. 2011. Significant efflux of carbon dioxide from streams and rivers in the United States. Nat. Geosci. **4**: 839–842. doi:10.1038/ngeo1294

Cole, J. J., and others. 2007. Plumbing the global carbon cycle: Integrating inland waters into the terrestrial carbon budget. Ecosystems **10**: 172–185. doi:10.1007/s10021-006-9013-8

DeGrandpre, M. D., T. R. Hammar, S. P. Smith, and F. L. Sayles. 1995. In situ measurements of seawater pCO2. Limnol. Oceanogr. **40**: 969–975. doi:10.4319/lo.1995.40.5.0969

Dickson, A. G., C. L. Sabine, and J. R. Christian [eds.]. 2007. Guide to best practices for ocean CO2 measurements, 191 p. PICES Special Publication 3.

Fietzek, P., B. Fiedler, T. Steinhoff, and A. Körtzinger. 2013. In situ quality assessment of a novel underwater pCO2 sensor based on membrane equilibration and NDIR spectrometry. J. Atmos. Oceanic Technol. **31**: 181–196. doi:10.1175/JTECH-D-13-00083.1

Frankignoulle, M. 1988. Field measurements of air-sea CO2 exchange. Limnol. Oceanogr. **33**: 313–322. doi:10.4319/lo.1988.33.3.0313

Frankignoulle, M., and A. V. Borges. 2001. Direct and indirect pCO2 measurements in a wide range of pCO2 and salinity values (The Scheldt Estuary). Aquat. Geochem. **7**: 267–273. doi:10.1023/A:1015251010481

Friederich, G. E., P. G. Brewer, R. Herlien, and F. P. Chavez. 1995. Measurement of sea surface partial pressure of C02 from a moored buoy. Deep-Sea Res. Part I Oceanogr. Res. Pap. **42**: 1175–1186. doi:10.1016/0967-0637(95)00044-7

Hales, B., and T. Takahashi. 2004. High-resolution biogeochemical investigation of the Ross Sea, Antarctica, during

the AESOPS (U. S. JGOFS) Program. Global Biogeochem. Cycles **18**: GB3006. doi:10.1029/2003GB002165

Hanson, P. C., D. L. Bade, S. R. Carpenter, and T. K. Kratz. 2003. Lake metabolism: Relationships with dissolved organic carbon and phosphorus. Limnol. Oceanogr. **48**: 1112–1119. doi:10.4319/lo.2003.48.3.1112

Hoppe, C. J. M., G. Langer, S. D. Rokitta, D. A. Wolf-Gladrow, and B. Rost. 2012. Implications of observed inconsistencies in carbonate chemistry measurements for ocean acidification studies. Biogeosciences **9**: 2401–2405. doi:10.5194/bg-9-2401-2012

Hunt, C. W., J. E. Salisbury, and D. Vandemark. 2011. Contribution of non-carbonate anions to total alkalinity and overestimation of pCO2 in New England and New Brunswick rivers. Biogeosciences **8**: 3069–3076. doi:10.5194/bg-8-3069-2011

Hunt, C. W., J. E. Salisbury, and D. Vandemark. 2013. CO2 input dynamics and air–sea exchange in a large New England estuary. Estuaries Coast. **37**: 1078–1091. doi:10.1007/s12237-013-9749-2

Johnson, M. S., M. F. Billett, K. J. Dinsmore, M. Wallin, K. E. Dyson, and R. S. Jassal. 2010. Direct and continuous measurement of dissolved carbon dioxide in freshwater aquatic systems—method and applications. Ecohydrology **3**: 68–78. doi:10.1002/eco.95

Laruelle, G. G., R. Lauerwald, B. Pfeil, and P. Regnier. 2014. Regionalized global budget of the CO2 exchange at the air-water interface in continental shelf seas. Global Biogeochem. Cycles **28**: 1199–1214. doi:10.1002/2014GB004832

Laruelle, G. G., R. Lauerwald, J. Rotschi, P. A. Raymond, J. Hartmann, and P. Regnier. 2015. Seasonal response of air–water CO2 exchange along the land–ocean aquatic continuum of the northeast North American coast. Biogeosciences **12**: 1447–1458. doi:10.5194/bg-12-1447-2015

Lewis, E. 1980. The practical salinity scale 1978 and its antecedents. IEEE J. Ocean. Eng. **5**: 3–8. doi:10.1109/JOE.1980.1145448

McDonald, C. P., E. G. Stets, R. G. Striegl, and D. Butman. 2013. Inorganic carbon loading as a primary driver of dissolved carbon dioxide concentrations in the lakes and reservoirs of the contiguous United States. Global Biogeochem. Cycles **27**: 285–295. doi:10.1002/gbc.20032

Newton, J. A., R. A. Feely, E. B. Jewett, P. Williamson, and J. Mathis. 2015. Global ocean acidification observing network: Requirements and governance plan, 2nd ed, GOA-ON. Available from http://www.goa-on.org/docs/GOA-ON_plan_print.pdf

Park, P. K. 1969. Oceanic $CO_2$ system: An evaluation of ten methods of investigation. Limnol. Oceanogr. **14**: 179–186. doi:10.4319/lo.1969.14.2.0179

Raymond, P. A., N. F. Caraco, and J. J. Cole. 1997. Carbon dioxide concentration and atmospheric flux in the Hudson River. Estuaries **20**: 381–390. doi:10.2307/1352351

Raymond, P. A., and others. 2013. Global carbon dioxide emissions from inland waters. Nature **503**: 355–359. doi:10.1038/nature12760

Signorini, S. R., and others. 2013. Surface ocean pCO2 seasonality and sea-air CO2 flux estimates for the North American east coast. J. Geophys. Res. Oceans **118**: 5439–5460. doi:10.1002/jgrc.20369

Takahashi, T. 1961. Carbon dioxide in the atmosphere and in Atlantic Ocean water. J. Geophys. Res. **66**: 477–494. doi:10.1029/JZ066i002p00477

Vandemark, D., J. E. Salisbury, C. W. Hunt, S. M. Shellito, J. D. Irish, W. R. McGillis, C. L. Sabine, and S. M. Maenner. 2011. Temporal and spatial dynamics of CO2 air-sea flux in the Gulf of Maine. J. Geophys. Res. **116**: C01012. doi:10.1029/2010JC006408

Wang, Z. A., D. J. Bienvenu, P. J. Mann, K. A. Hoering, J. R. Poulsen, R. G. M. Spencer, and R. M. Holmes. 2013. Inorganic carbon speciation and fluxes in the Congo River. Geophys. Res. Lett. **40**: 511–516. doi:10.1002/grl.50160

Wanninkhof, R., and K. Thoning. 1993. Measurement of fugacity of CO2 in surface water using continuous and discrete sampling methods. Mar. Chem. **44**: 189–204. doi:10.1016/0304-4203(93)90202-Y

Weiss, 1981. Determinations of carbon dioxide and methane by dual catalyst flame ionization chromatography and nitrous oxide by electron capture chromatography 19: 611–616. doi:10.1093/chromsci/19.12.611

Yasuda, T., S. Yonemura, and A. Tani. 2012. Comparison of the characteristics of small commercial NDIR CO2 sensor models and development of a portable CO2 measurement device. Sensors **12**: 3641–3655. doi:10.3390/s120303641

## Acknowledgments

Associate Editor Michael Degrandpre, reviewer Wiley Evans, and one anonymous reviewer provided essential criticism and feedback which greatly helped shape this work. Lauren Koenig provided a thoughtful review of an early version of this paper. Funding for this work was provided by NOAA Award NA15NOS0120155, NOAA/NERACOOS Award A002004, and EPSCoR Ecosystems and Society Award EPS-1101245. Partial funding was provided by the New Hampshire Agricultural Experiment Station. This is Scientific Contribution Number 2693. This work was supported by the USDA National Institute of Food and Agriculture McIntire-Stennis Project 1006760).

## Conflict of Interest

None declared.

*Submitted 05 October 2016*
*Revised 15 November 2016*
*Accepted 17 November 2016*

*Associate editor: Mike DeGrandpre*